Pharmacological characterization of novel heteromeric GluCl subtypes from C. elegans and parasitic nematodes

Nicolas Lamassiaude, Elise Courtot, Angélique Corset, Claude L. Charvet, Cédric Neveu

eppendorf

Reach Your 100%

Your success is our purpose

Your time is precious not only in terms of cost. However, a drug's journey from concept to patient takes years. You need to rely on products and services that ensure maximum efficiency at every step.

Our high-quality solutions are all engineered around the kind of functionality and intuitive performance necessary to speed up workflows, secure reproducibility, and accelerate the desired results.

Let's work together to make our world a better place.

www.eppendorf.com/pharma

Received: 19 March 2021 | Revised: 30 August 2021 | Accepted: 1 September 2021

DOI: 10.1111/bph.15703

RESEARCH ARTICLE

Pharmacological characterization of novel heteromeric GluCl subtypes from *Caenorhabditis elegans* and parasitic nematodes

Nicolas Lamassiaude | **Elise Courtot** | **Angélique Corset** | **Claude L. Charvet** | **Cédric Neveu**

INRAE, Université de Tours, ISP, Nouzilly, France

Correspondence
Claude L. Charvet and Cédric Neveu, INRAE, Université de Tours, ISP, F-37380 Nouzilly, France.
Email: claude.charvet@inrae.fr; cedric.neveu@inrae.fr

Funding information
RTR Fédération de Recherche en Infectiologie; Region Centre-Val de Loire, France; Animal Health Division of INRAE

Background and Purpose: Macrocyclic lactones are the most widely used broad-spectrum anthelmintic drugs for the treatment of parasitic nematodes affecting both human and animal health. Macrocyclic lactones are agonists of the nematode glutamate-gated chloride channels (GluCls). However, for many important nematode species, the GluCls subunit composition and pharmacological properties remain largely unknown. To gain new insights into GluCl diversity and mode of action of macrocyclic lactones, we identified and pharmacologically characterized receptors made of highly conserved GluCl subunits from the model nematode *Caenorhabditis elegans*, the human filarial nematode *Brugia malayi* and the horse parasite *Parascaris univalens*.

Experimental Approach: AVR-14, GLC-2, GLC3 and GLC-4 are the most conserved GluCl subunits throughout the Nematoda phylum. For each nematode species, we investigated the ability of these subunits to form either homomeric or heteromeric GluCls when expressed in *Xenopus laevis* oocytes and carried out detailed pharmacological characterization of the functional channels.

Key Results: A total of 14 GluCls were functionally reconstituted, and heteromers formation was inferred from pharmacological criteria. The GLC-2 subunit plays a pivotal role in the composition of heteromeric GluCls in nematodes. We also found a novel GluCl subtype, combining GLC-2/GLC-3 subunits, for which a high concentration of the anthelmintics ivermectin and moxidectin reversibly potentiates glutamate-induced response.

Conclusion and Implications: This study brings new insights into the diversity of GluCl subtypes in nematodes and promotes novel drug targets for the development of the next generation of anthelmintic compounds.

Abbreviation: GluCl, glutamate-gated chloride channel.

1 | INTRODUCTION

The phylum Nematoda is divided into five major clades (I to V) that include free living and parasitic species affecting human, animal and plant health (Blaxter & Koutsovoulos, 2015; Blaxter et al., 1998). Among these parasitic nematodes, *Filarioidea* and *Ascaridoidea* belonging to clade III are considered as those most affecting both humans and animals (Pullan et al., 2014). In this study, we focus our research on two parasitic nematode species representative of human filarids and animal ascarids: *Brugia malayi*, a human lymphatic filarid which is the causative agent of chronic elephantiasis in south and south-east Asia (Global programme to eliminate lymphatic filariasis: progress report, 2016, 2017), and *Parascaris* sp., which is responsible for equine ascaridiosis (Reinemeyer & Nielsen, 2009; Salle et al., 2020).

Without effective vaccines or alternative strategies (Matthews et al., 2016), the use of anthelmintic treatments remains the standard control strategy for parasitic nematodes. Among the available anthelmintic drugs, the broad-spectrum macrocyclic lactones (MLs) are highly effective and are widely used in human and veterinary medicine (Laing et al., 2017). The macrocyclic lactones include avermectins (**ivermectin**, doramectin, eprinomectin, abamectin, selamectin and emamectin and milbemycins (moxidectin, milbemycin-oxime and nemadectin) that are potent against both endoparasites and ectoparasites (Campbell, 2012). The morbidity and socio-economic impact of human lymphatic filariasis motivated control programmes led by the World Health Organization (WHO) with ivermectin as a spearhead of eradication operations (Ramaiah & Ottesen, 2014). For the control of *Parascaris* sp. infestations, currently, three drug classes have marketing approval including benzimidazoles, pyrantel and the macrocyclic lactones (ivermectin and moxidectin), with the last being the most widely used family. Unfortunately, because of the intensive use of macrocyclic lactones, treatment failures and resistant parasites have been reported worldwide (Kaplan & Vidyashankar, 2012; Peregrine et al., 2014). In this context, a better understanding of the mode of action of the macrocyclic lactones is essential for the development of novel treatment strategies.

In the free-living model nematode *Caenorhabditis elegans*, macrocyclic lactones act as allosteric modulators of glutamate-gated chloride channels (GluCls) (Cully et al., 1994). Exposure to the macrocyclic lactones hyperpolarizes the cell membrane and inhibits neurotransmission (Cook et al., 2006; Dent et al., 1997; Holden-Dye & Walker, 2006), leading to a stationary paralysis of the worms (Dent et al., 2000; Hernando & Bouzat, 2014). GluCls are made of five subunits combining together to form either homomeric or heteromeric receptors (Degani-Katzav et al., 2016; Hibbs & Gouaux, 2011). In order to investigate the subunit composition and the pharmacological properties of recombinant nematode GluCls, the *Xenopus laevis* oocyte has proved to be an efficient heterologous expression system (Bianchi & Driscoll, 2006).

In *C. elegans*, six GluCl genes were identified and named *avr-14* (Dent et al., 2000; McCavera et al., 2009), *avr-15* (Dent et al., 1997; Vassilatis et al., 1997), *glc-1* (Cully et al., 1994), *glc-2* (Cully et al., 1994; Vassilatis et al., 1997), *glc-3* (Horoszok et al., 2001) and *glc-4* (Cully et al., 1996). With the exception of GLC-4, all the subunits are able to form functional homomeric receptors when expressed in *X. laevis* oocytes. All functional homomeric receptors are ivermectin-sensitive, with the exception of Cel-GLC-2 (Cully et al., 1994). Interestingly, it has been reported that the *C. elegans* GLC-2 subunit co-assembles with Cel-GLC-1 (Cully et al., 1994) or Cel-AVR-15 (Vassilatis et al., 1997) to form two distinct ivermectin-sensitive heteromeric GluCl subtypes with different pharmacological properties.

In contrast to *C. elegans*, few functional GluCls have been characterized so far in parasitic nematodes. The AVR-14B subunit was reported to form functional homomeric GluCls in *Haemonchus contortus* (Atif et al., 2017; Cheeseman et al., 2001; McCavera et al., 2009), *Cooperia oncophora* (Njue et al., 2004) and *Dirofilaria immitis* (Yates & Wolstenholme, 2004). Interestingly, in *C. oncophora* and *H. contortus*, GLC-2 also combined with AVR-14B to form a heteromeric GluCl subtype sensitive to ivermectin (Atif et al., 2019; Njue et al., 2004). As GluCl investigations have mainly focused on clade V nematodes, GluCl diversity and the mode of action of macrocyclic lactones remain poorly understood in human and animal parasitic nematodes from the clade III.

In the present study, we reasoned that GluCls composed of the highly conserved AVR-14, GLC-2, GLC-3 and GLC-4 subunits could be involved in the broad-spectrum activity of macrocyclic lactones on

What is already known

- Macrocyclic lactones are the most widely used anthelmintics for the control of parasitic nematodes.
- Macrocyclic lactones act as agonists of nematode pentameric glutamate-sensitive chloride channels (GluCls).

What does this study adds

- New heteromeric GluCls from parasites as molecular targets for structurally different macrocyclic lactones.
- Characterization of a novel nematode GluCl subtype on which macrocyclic lactones potentiate glutamate-induced responses.

What is the clinical significance

- Identification of targets of macrocyclic lactones in two of the most important parasitic nematode groups.
- New targets for rational drug screening for the identification of next generation anthelmintic compounds.

nematodes. Using *Xenopus* oocytes, we reconstituted a panel of functional homomeric and heteromeric GluCls from *C. elegans*, *B. malayi* and *Parascaris univalens*. We characterized a novel heteromeric GLC-2/GLC-3 GluCl subtype not previously described. Finally, our results provide new insights on the pharmacology of nematode GluCl subtypes as well as the mode of action of a wide range of macrocyclic lactones, thus highlighting the heteromeric GluCls as potential contributors to sensitivity to macrocyclic lactones in nematodes.

2 | METHODS

2.1 | Nematodes

C. elegans used in this study are Bristol N2 wild-type strain worms supplied by the *Caenorhabditis* Genetics Center (CGC), St. Paul, MN, USA, which is funded by the NIH Office of Research Infrastructure Programs (P40 OD010440). *B. malayi* L4 larvae were supplied by NIH/NIAID Filariasis Research Reagent Resource Center, University of Georgia, Athens, GA, USA (www.filariasiscenter.org). Adult *P. univalens* were collected in faeces of naturally infested foals from UEPAO (Experimental Unit of Orfrasière Animal Physiology, INRAE Centre Val de Loire, Nouzilly 37380, France). Adult worms were collected, 50 h after a treatment with ivermectin. All samples were stored at −80°C in RNAlater solution (Ambion, Austin, TX, USA) before use. Note that because *Parascaris equorum* and *P. univalens* are morphologically identical, we confirmed the species status by karyotyping *Parascaris* eggs before collecting the adult worms. Briefly, parascaris eggs were extracted from faecal samples from four foals from the UEPAO. Faeces were mixed with tap water and deposited on two sieves stacked in order of size (125 μm on the top and 63 μm on the bottom). Eggs were collected and washed with tap water on the 60-μm sieve. Karyotyping was performed as described previously (Martin et al., 2018). Whereas *P. univalens* has one pair of chromosome, *P. equorum* has two (Nielsen et al., 2014). *P. univalens* was identified as the single *Parascaris* species present in the naturally infected foals from UEPAO, because all eggs had a single pair of chromosomes (Figure S1).

2.2 | Molecular biology

Total RNA was extracted from a pool of adults for *C. elegans* and from a pool of L4 larvae for *B. malayi*. For *P. univalens*, total RNA was extracted from the head of a single worm, including pharynx. Total RNA was isolated with Trizol reagent (Invitrogen, Carlsbad, CA, USA) as previously described (Charvet et al., 2018). cDNA synthesis was performed with 0.5–5 μg of total RNA using the Maxima H minus Reverse Transcriptase kit (Thermo Scientific, Waltham, MA, USA) according to the manufacturer's recommendations.

PCR amplifications were performed according to the manufacturer's recommendations with the Phusion High Fidelity Polymerase (New England BioLabs, Ipswich, MA, USA) using cDNA as template. Full-length coding sequences were cloned into the transcription vector pTB-207, and RACE-PCR product were cloned into pGEM-T (Promega, Madison, WI, USA). Eurofins Genomics (Luxembourg) sequenced all constructs. Sequences of Cel-AVR-14B (CAA04170), Cel-GLC-2 (AAA50786), Cel-GLC-3 (CAB51708) and Cel-GLC-4 (NP_495489.2) from *C. elegans* were available on GenBank as well as Pun-AVR-14B (ABK20343) subunit coding sequence from *P. univalens*. Using the GluCl sequences of *C. elegans* and Pun-AVR-14B as queries, tBLASTn searches in WormbaseParasite databank (https://parasite.wormbase.org/Tools/Blast?db=core) allowed the identification of full-length coding sequence of GluCls from *B. malayi* (Bma-GLC-2: XM_001893073.1; Bma-GLC-4: XM_001900205.1; Bma-AVR-14B: supercontig:Bmal-4.0:Bm_v4_Chr3_scaffold_001:1374074:1388079:1; Bma-GLC-3: Bmal-4.0:Bm_v4_Chr4_scaffold_001:1513094:1542759:-1) and partial sequences of GluCls from *P. univalens* (Pun-GLC-2: NODE_2545302; Pun-GLC-3: NODE_2129897 and NODE_2250308; Pun-GLC-4: NODE_1817943, NODE_2402242 and NODE_2418647). Primer sequences designed for RACE PCR and amplification of the full-length coding sequences of each subunit are provided in Table S1. For GluCl subunits of *P. univalens*, the corresponding 5′ and 3′ cDNA ends were obtained by nested RACE-PCR experiments as previously described (Courtot et al., 2015). The full-length coding sequence of all GluCl subunits was obtained by nested PCR using the proofreading Phusion High-Fidelity DNA Polymerase (Thermo Scientific, Waltham, MA, USA). Subsequently, PCR products were cloned into the transcription vector pTB-207 as previously described (Charvet et al., 2018). Recombinant constructs were sequence checked and linearized with MlsI, PaeI or PacI restriction enzymes (Thermo Scientific, Waltham, MA, USA) depending on the construct. Linearized plasmids were used as DNA templates for cRNA synthesis using the mMessage mMachine T7 transcription kit (Ambion, Austin, TX, USA). cRNAs were precipitated with lithium chloride and were resuspended in a suitable volume of RNAse-free water and stored at −20°C before use.

2.3 | Sequence analysis and phylogeny

Deduced amino-acid sequences of GluCl subunits from *B. malayi*, *C. elegans*, *H. contortus* and *P. univalens* were aligned using the MUSCLE algorithm included in the Seaview 5.0.4 package (Gouy et al., 2010). Percentage of identity between deduced amino acids of mature protein without peptide signal was obtained using the EMBOSS Needle software (Madeira et al., 2019). Signal peptide predictions were performed using the SignalP 3.0 server (Bendtsen et al., 2004), and membrane-spanning regions were predicted using the SMART server (Schultz et al., 1998). Phylogenetic analyses were performed on coding sequences predicted from genomic data available in databases or cloned cDNA sequences when available. Maximal likelihood phylogeny reconstruction was performed using PhyML V3.1 included in the Seaview 5.0.4 package. Significance of the internal tree branches was estimated using bootstrap with 100 replicates. The tree was edited using the FigTree software (http://tree.bio.ed.ac.uk/software/figtree/). The sequences used in this study are available

on GenBank under the following accession numbers: *B. malayi* (Bma): AVR-14B (MW196269), GLC-2 (MW196266), GLC-3 (MW196267), GLC-4 (MW196268); *C. elegans* (Cel): AVR-14B (MW196270), AVR-15A (CAA04171), AVR-15B (CAA04170), GLC-1 (AAA50785), GLC-2 (AAA50786), GLC-3 (CAB51708), GLC-4 (NP_495489.2), UNC-49B (AAD42383); *H. contortus* (Hco): AVR-14B (CAA74623), GLC-2 (CAA70929); *P. univalens* (Pun): AVR-14B (MW187941), GLC-2 (MW187938), GLC-3 (MW187939), GLC-4 (MW187940).

2.4 | Electrophysiological recording in *X. laevis* oocytes

Distinct batches of defolliculated *X. laevis* oocytes were purchased from Ecocyte Bioscience (Dortmund, Germany) and micro-injected using the Drummond nanoject II microinjector with 72 ng of cRNA when subunits were expressed singly or with 50 ng for each subunit when expressed in combination (1:1 ratio). Two-electrode voltage-clamp recordings were performed at a holding potential of −80 mV to assess the expression of the GluCl channels as previously described (Lamassiaude et al., 2021). Currents were recorded and analysed using the pCLAMP 10.4 package (Molecular Devices, San Jose, CA, USA). All recordings were performed at room temperature (20 ± 1°C).

Dose–responses relationships for glutamate were carried out by challenging oocytes with 5–10 s of application of increasing concentration of glutamate (from 1 μM up to 30 mM, depending on the receptor) with 2-min washing steps with Ringer solution between each application. The peak current values were normalized to the maximum response obtained with a saturating concentration of glutamate. Comparison of the effects of the macrocyclic lactones on receptors was performed as described previously (Njue et al., 2004; Yates & Wolstenholme, 2004). Briefly, 1-mM glutamate was first perfused on the oocytes as a reference peak current (maximum response) before application of a macrocyclic lactone at 1 μM for 5 s. Current responses were normalized to the maximum current amplitude obtained with 1-mM glutamate. For Pun-GLC-2/GLC-3, the potentiating effect of macrocyclic lactones was evaluated by a first application of each macrocyclic lactone alone for 5 s, followed by the co-application with 100-μM glutamate for 5 s. Then, in order to monitor a potential reversible effect, the oocytes were washed for 2 min with Ringer solution before a subsequent application of 100-μM glutamate. The observed responses were normalized to the response induced by 100-μM glutamate (corresponding approximately to the glutamate EC_{50} for Pun-GLC-2/GLC-3) alone, performed prior to challenging with the macrocyclic lactone.

2.5 | Data and statistical analysis

The data and statistical analysis comply with the recommendations of the British Journal of Pharmacology on experimental design and analysis in pharmacology (Curtis et al., 2018). Each experiment corresponds to current recordings made on at least five different oocytes (n) from at least five distinct defolliculated egg batches. Only one drug was tested on each oocyte. In order to minimize variation, current amplitudes were normalized to the maximal effect obtained with a saturating glutamate concentration. None of the experiments were blinded or randomized as pharmacological characterization of the GluCls were performed with a set of selected drugs. The group sizes varied with the type of experiment performed. In order to investigate putative functional recombinant homomeric or heteromeric GluCls, responsive or not to 1-mM glutamate, at least eight recordings were performed on independent oocytes for each putative receptor. For the heteromeric GluCls selected for further pharmacological characterizations (i.e., AVR-14B/GLC-2 and GLC-2/GLC-3), expression robustness (variability between oocytes) was evaluated with at least 17 recordings performed on independent oocytes. For each GluCl subtype, glutamate dose–response and agonist/antagonist experiments were performed on at least five independent oocytes. Statistical analysis was undertaken only for studies where each group size was at least $n = 5$. All statistical analyses were performed using the software R (v3.6.1). All data were tested for normality with a Shapiro–Wilk test, and outliers were included in data analysis and presentation. When data followed a normal distribution, statistical significance was calculated using one-way ANOVA with post hoc Tukey's HSD test using the Bonferroni correction for comparisons among more than two groups (Figure 4). Post hoc tests were run only if F achieved $P < 0.05$ and there was no significant variance in homogeneity using Levene's test. $P < 0.05$ was considered statistically significant. The Mann–Whitney test was performed to compare the effect of a single drug on similar receptors from distinct nematode species (Figure 6). For paired data (Figure 7), a non-parametric Friedman test followed by a post hoc Conover multiple comparison test using the Bonferroni correction was used. Dose–response data were modelled as a log-logistic regression with two parameters, that is, the curve slope and the associated EC_{50} concentration, using the drc package v3.0-1.

2.6 | Materials

Glutamate, piperazine and the macrocyclic lactones (selamectin, ivermectin, doramectin, emamectin, eprinomectin, abamectin and moxidectin) were purchased from Sigma-Aldrich (Saint-Quentin Fallavier, France). These macrocyclic lactones were first dissolved in DMSO at 10 mM and then diluted in Ringer solution to the required concentration with a final concentration of DMSO which did not exceed 1%. Glutamate was directly prepared in recording solution.

2.7 | Nomenclature of targets and ligands

Key protein targets and ligands in this article are hyperlinked to corresponding entries in the IUPHAR/BPS Guide to PHARMACOLOGY http://www.guidetopharmacology.org and are permanently archived in the Concise Guide to PHARMACOLOGY 2021/22 (Alexander, Mathie et al., 2021).

3 | RESULTS

3.1 | Four distinct GluCl subunits are conserved between *C. elegans*, *B. malayi* and *P. univalens*

Searches for homologues of GluCl subunit encoding genes from *C. elegans* (i.e., *glc-1*, *glc-2*, *glc-3*, *glc-4*, *avr-14* and *avr-15*) (Cully et al., 1994; Dent et al., 1997, 2000; Horoszok et al., 2001; Vassilatis et al., 1997) in *B. malayi* and *P. univalens* genomic/transcriptomic databases allowed the identification of four independent sequences corresponding to putative homologues of *avr-14*, *glc-2*, *glc-3* and *glc-4* from both species. In contrast, homologues could not be found in *B. malayi* and *P. univalens* for *glc-1* or *avr-15*. The full-length cDNAs of *avr-14*, *glc-2*, *glc-3* and *glc-4* from the three nematode species were cloned, sequenced and submitted to GenBank under the accession numbers provided in Section 2. All GluCl subunits identified including AVR-14B, GLC-2, GLC-3 and GLC-4 from *C. elegans*, *B. malayi* and *P. univalens* present the typical characteristics of a Cys-loop receptor subunit. This includes a predicted signal peptide in the extracellular N-terminal part (with the exception of Bma-GLC-2), the first Cys-loop domain specific for **ligand-gated ion channels** (LGIC) composed of two cysteines that are 13 amino-acid residues apart, the second Cys-loop domain found in GluCls, and four transmembrane domains (TM1–4) (Figures S2 and S3). In comparison with *C. elegans*, the GluCl-deduced amino-acid sequences of *B. malayi* and *P. univalens*, respectively, show an identity of 78.4% and 80.3% for AVR-14B, 64.1% and 67.2% for GLC-2, 66.5% and 67.8% for GLC-3 and 64.8% and 66.6% for GLC-4 (Table S2). A phylogenetic analysis including GluCl sequences from *C. elegans* (Cel), *B. malayi* (Bma), *H. contortus* (Hco) and *P. univalens* (Pun) confirmed the orthologous relationship of the parasitic subunit sequences with their respective counterparts in *C. elegans* (Figure 1). The identified sequences were named according to the nomenclature proposed by Beech et al. (2010). The full-length cDNA sequences of all the subunits (including Bma-GLC-2 lacking a predicted signal peptide) were cloned into a transcription vector for subsequent analysis.

3.2 | *C. elegans* GluCl subunits are more prone to reconstitute robustly expressed homomeric glutamate-sensitive receptors than their parasite counterparts

In order to test the ability of *C. elegans*, *B. malayi* and *P. univalens* GluCl subunits to form functional homomeric receptors, their respective cRNAs (*avr-14b*, *glc-2*, *glc-3* and *glc-4*) were injected singly into *X. laevis* oocytes. Four days after injection, currents elicited by 1-mM glutamate application were recorded using the two-electrode voltage-clamp technique (Figure 2a).

Here, the *C. elegans* AVR-14B, GLC-2 and GLC-3 GluCl subunits were used as positive controls as their ability to form functional glutamate-sensitive homomeric channels has been previously

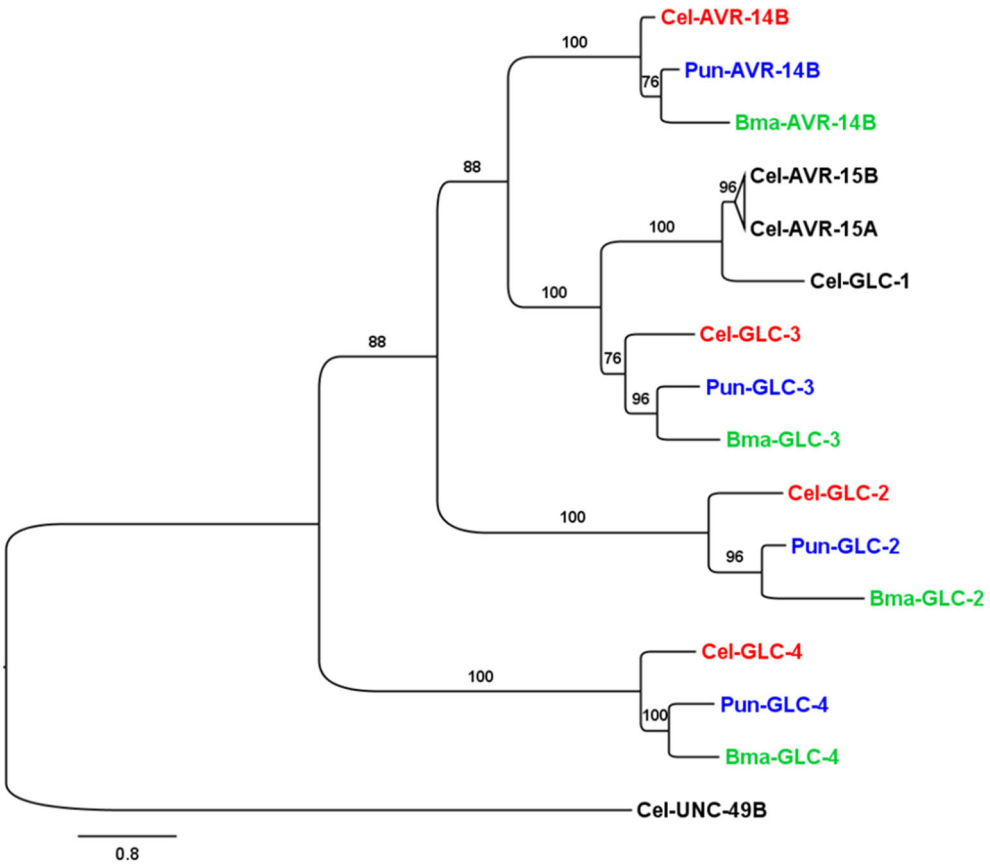

FIGURE 1 Maximal likelihood tree generated with GluCl subunit deduced amino-acid sequences from *Brugia malayi* (Bma), *Caenorhabditis elegans* (Cel) and *Parascaris univalens* (Pun). The bootstrap values (100 replicates) are indicated at each node. Scale bar represents the number of substitutions per site. Accession numbers for the sequences used in this analysis are provided in Section 2. The *B. malayi*, *C. elegans* and *P. univalens* GluCl subunit sequences investigated in the present study are highlighted in green, red and blue, respectively. The GABA receptor subunit UNC-49B from *C. elegans* was used as an outgroup

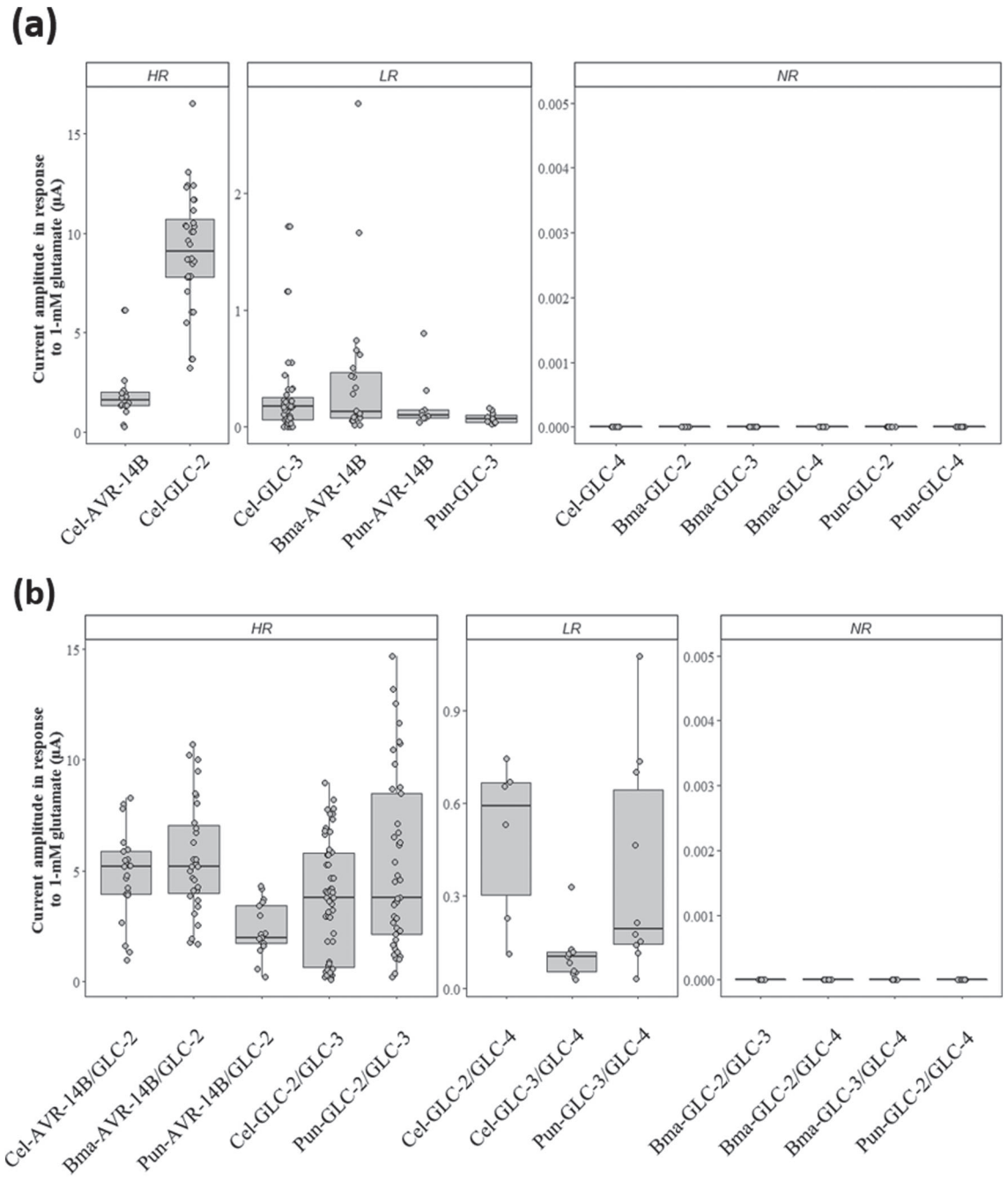

FIGURE 2 Functional expression of GluCl subunits from *Caenorhabditis elegans*, *Brugia malayi* and *Parascaris univalens* in *Xenopus laevis* oocytes. (a,b) Box plots depict response elicited by 1-mM glutamate application on *Xenopus* oocytes expressing homomeric (a) or heteromeric (b) receptors for *C. elegans*, *B.* malayi and *P. univalens*. HR (high response) corresponds to subunit combinations that led to robust expression of receptors responding to 1-mM glutamate with peak current in the µA range. LR (low response) corresponds to subunit combinations that respond to 1-mM glutamate with moderate currents in the nA range. NR (no response) corresponds to combinations that did not respond to 1-mM glutamate application

reported (Cully et al., 1994; Dent et al., 2000; Horoszok et al., 2001; McCavera et al., 2009). In our hands, Cel-AVR-14B or Cel-GLC-2 alone formed functional homomeric receptors with robust glutamate-elicited currents in the µA range: (as medians) 1.6 µA ($n = 16$) and 9.1 µA ($n = 32$) for Cel-AVR-14B and Cel-GLC-2, respectively. Although Cel-GLC-3 was also able to form functional receptors, the currents elicited by 1-mM glutamate were in the nA range (median, 176 nA, $n = 50$). Finally, no 1-mM glutamate-induced current was observed on oocytes injected with Cel-GLC-4 cRNA ($n = 18$). These results are in agreement with previous studies (Cully et al., 1994, 1996; Dent et al., 2000; Horoszok et al., 2001).

Unlike *C. elegans*, where three out of four GluCl subunits formed functional homomeric receptors, for *B. malayi*, only the expression of AVR-14B in oocytes allowed the recording of reliable currents

(median, 134 nA, $n = 23$). For *P. univalens*, AVR-14B and GLC-3 reconstituted functional homomeric receptors, with 1-mM glutamate-elicited median currents of 103.6 nA ($n = 9$) and 70 nA ($n = 11$), respectively. Finally, in oocytes injected with *Bma-glc-2* ($n = 11$), *Pun-glc-2* ($n = 11$), *Bma-glc-3* ($n = 14$), *Bma-glc-4* ($n = 13$) or *Pun-glc-4* ($n = 12$), 1-mM glutamate application did not produce detectable responses.

3.3 | GLC-2 plays a pivotal role in heteromeric GluCl composition

Because previous studies highlighted the involvement of GLC-2 in heteromeric GluCls (Atif et al., 2019; Cully et al., 1994; Vassilatis et al., 1997), oocytes expressing a combination of GLC-2 with AVR-14B, GLC-3 or GLC-4 were challenged with 1-mM glutamate (Figure 2b).

Firstly, we investigated the AVR-14B/GLC-2 combination for the three different nematode species. As expected, the co-expression of both subunit cRNAs from *C. elegans* led to the robust expression of GluCls with a median current amplitude of 5.2 μA ($n = 21$). Surprisingly, the *B. malayi* AVR-14B/GLC-2 combination led to the robust expression of receptors responsive to 1-mM glutamate with a median current amplitude of 5.1 μA ($n = 31$), corresponding to a 38-fold increase, in comparison with the homomeric receptor made of Bma-AVR-14B alone. Note that such a result was unexpected as Bma-GLC-2 lacks a predicted signal peptide. The *P. univalens* AVR-14B/GLC-2 combination also led to the robust expression of functional receptors with 1-mM glutamate-elicited currents of 2.0 μA ($n = 17$), corresponding to a 19-fold increase in comparison with Pun-AVR-14B alone. These first results indicated that AVR-14B and GLC-2 could assemble into functional heteromeric receptors potentially distinguishable from homomeric receptors.

Secondly, we tested the ability of the GLC-2 subunit to assemble with GLC-3. For the *C. elegans* GLC-2/GLC-3 combination, we recorded strong currents elicited by 1-mM glutamate (median 3.8 μA, $n = 59$). Strikingly, for *P. univalens*, the combination of GLC-2/GLC-3 also led to the robust expression of glutamate-sensitive receptors with a median current amplitude of 3.8 μA ($n = 45$), corresponding to a 54-fold increase in comparison with the currents recorded on the Pun-GLC-3 homomeric receptor. These results suggested that Pun-GLC-2 and Pun-GLC-3 could assemble into heteromeric receptors. In contrast, for *B. malayi*, the GLC-2/GLC-3 combination failed to give rise to a functional receptor responsive to 1-mM glutamate ($n = 8$). Because Bma-GLC-2 has proved to be functional in combination with AVR-14B, we addressed the functionality of Bma-GLC-3 by co-injecting *Bma-glc-3* together with *Pun-glc-2* in *Xenopus* oocytes. The recordings of glutamate-elicited currents in the μA range resulting from a functional chimeric receptor made of Pun-GLC-2 and Bma-GLC-3 confirmed that Bma-GLC-3 is a functional subunit (Figure S4). Therefore, the Bma-GLC-2 and Bma-GLC-3 subunits do not assemble to form a functional heteromeric channel responsive to 1-mM glutamate although both are functional subunits.

Thirdly, we tested the combination of GLC-2 with GLC-4 for all species. For the *C. elegans* GLC-2/GLC-4 combination, median currents of 592 nA ($n = 14$) were recorded, corresponding to a 15-fold decrease in comparison with Cel-GLC-2 alone. Note that such a reduction of glutamate-induced response has been previously reported, when Cel-GLC-2 was co-expressed with Cel-GLC-1 (Cully et al., 1994). In contrast with *C. elegans*, the *B. malayi* and the *P. univalens* GLC-2/GLC-4 combination failed to produce detectable glutamate responses ($n = 8$ and $n = 11$, respectively).

Finally, we tested the combination of GLC-3 with the GLC-4 subunit for all species. No currents could be recorded with 1-mM glutamate application on oocytes injected with Bma-GLC-3/GLC-4 ($n = 13$), although nA range currents were recorded for Cel-GLC-3/GLC-4 and for Pun-GLC-3/GLC-4. Taken together, these results highlight the role of GLC-2 from the three different species in the formation of glutamate-sensitive heteromeric receptors, including either AVR-14B or GLC-3.

3.4 | The AVR-14B/GLC-2 GluCl subtype is targeted by a wide range of MLs

In order to distinguish the putative Cel-AVR-14B/GLC-2 heteromeric receptor from the Cel-AVR-14B and Cel-GLC-2 homomeric channels, we determined their respective glutamate concentration–response curves. Glutamate EC_{50} values (shown as geometric means with 95% confidence intervals) of 112.2 (88.3 - 142.8) μM ($n = 5$), 214.7 (189 - 243.9) μM ($n = 5$) and 19.4 (17.2 - 22) μM ($n = 8$) were obtained for the Cel-AVR-14B, Cel-GLC-2 and Cel-AVR-14B/GLC-2 receptors, respectively (Figure 3a). Cel-AVR-14B/GLC-2 channels exhibited a significantly higher sensitivity for glutamate in comparison with the homomeric receptors formed by AVR-14B or GLC-2, with 5- and 10-fold lower EC_{50}, respectively. These results strongly support the view that Cel-AVR-14B and GLC-2 can combine to form a functional heteromeric GluCl receptor distinguishable from the respective homomers.

For *B. malayi*, we determined the glutamate EC_{50} values for Bma-AVR-14B and Bma-AVR-14B/GLC-2 but not for GLC-2 alone as it did not form a functional homomeric receptor responsive to 1-mM glutamate. For the AVR-14B homomeric channel, the glutamate EC_{50} value was 761.4 (618.2 - 937.7) μM ($n = 5$), whereas the EC_{50} of the Bma-AVR-14B/GLC-2 combination was 32.5 (24 - 44.1) μM ($n = 7$) (Figure 3b). This drastic shift of glutamate sensitivity (23-fold) provides strong evidence that AVR-14B and GLC-2 subunits from *B. malayi* associate to form a heteromeric GluCl subtype, distinct from the homomeric receptor composed of AVR-14B.

For the *P. univalens* homomeric AVR-14B receptor, the glutamate EC_{50} value could not be determined. Indeed, the application of high concentrations of glutamate only induced small currents that did not reached a plateau value. Note that even with 100-mM glutamate applications ($n = 7$), the receptor was not saturated. In sharp contrast, the co-injection of *avr-14B* and *glc-2* cRNAs led to the robust expression of a functional receptor with a

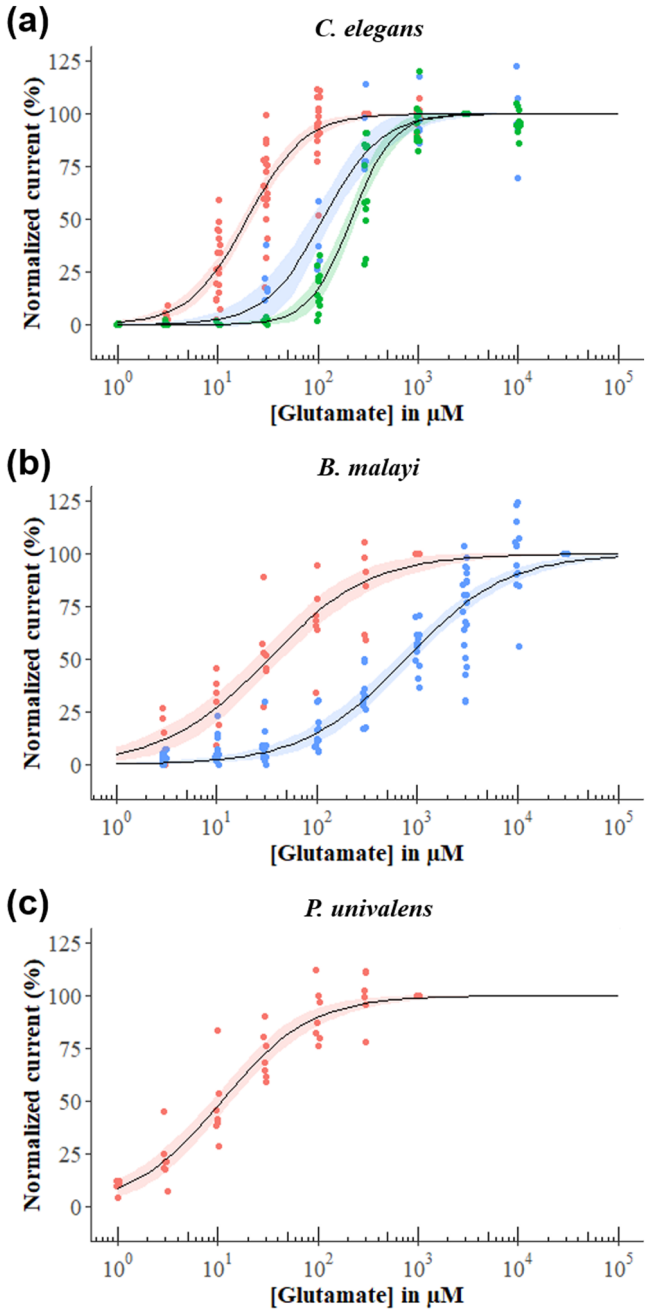

FIGURE 3 Glutamate concentration–response relationships for the AVR-14B/GLC-2 receptors from *Caenorhabditis elegans*, *Brugia malayi* and *Parascaris univalens*. Glutamate concentration–response curves for AVR-14B/GLC-2 (red), AVR-14B (blue) and GLC-2 (green) from C. elegans (a), B. malayi (b) and P. univalens (c). Current amplitudes were normalized to the maximal effect obtained with a saturating glutamate concentration. Solid line stands for the fitted log-logistic regression curve, and shaded area indicates 95% confidence interval. For both *C. elegans* and *B. malayi*, the glutamate EC_{50}s were significantly different ($P<0.05$) between the heteromeric AVR-14B/GLC-2 receptors and the respective homomeric AVR-14 and GLC-2 channels

glutamate EC_{50} value of 10.9 (8.8 – 13.6) µM ($n = 5$) (Figure 3c). Taken together, these results confirmed that Pun-AVR-14B/GLC-2 form a heteromeric GluCl.

Subsequently, in order to get new insights into their respective pharmacological properties, the heteromeric AVR-14B/GLC-2 GluCls from *C. elegans*, *B. malayi* and *P. univalens* were challenged with a wide range of marketed macrocyclic lactone compounds used as anthelmintic, insecticide or acaricide (abamectin, doramectin, emamectin, eprinomectin, ivermectin, moxidectin and selamectin (Figure 4 and Table 1). Recordings revealed that all the macrocyclic lactones tested in the present study acted as potent agonists on these receptors, inducing their permanent activation. Large currents were recorded in response to 1 µM for all the macrocyclic lactones tested. Representative currents induced by the application of macrocyclic lactones on oocytes expressing the AVR-14B/GLC-2 receptor from each species are presented in Figure 4a,c,e. As previously described, receptor activation by the macrocyclic lactones was not reversible and slower in comparison with glutamate. Interestingly, the insecticide emamectin was found to be more potent than the standard drug ivermectin on both Cel-AVR-14B/GLC-2 and Bma-AVR-14B/GLC-2. In contrast, no significant difference of sensitivity between ivermectin and the other macrocyclic lactones was observed on Pun-AVR-14B/GLC-2 (Figure 4b,d,f).

3.5 | GLC-2/GLC-3: A new functional heteromeric GluCl subtype with original pharmacological properties

In order to distinguish the putative Cel-GLC-2/GLC-3 heteromeric receptor from the Cel-GLC-2 and Cel-GLC-3 homomeric receptors, we compared their respective glutamate EC_{50} values (Figure 5a).

For Cel-GLC-2/GLC-3, the glutamate EC_{50} value was 46.8 (40.3 – 54.2) µM ($n = 5$), corresponding to a 4-fold reduction in comparison with the glutamate EC_{50} value previously determined for Cel-GLC-2 alone (214.7 (189 – 243.9) µM, $n = 5$) and a 40-fold reduction in comparison with the glutamate EC_{50} value of Cel-GLC-3 (1.9 ± 0.03 mM) previously reported by Horoszok et al. (2001). The shift in these EC_{50} values indicates that *C. elegans* GLC-2 and GLC-3 can combine to form a new GluCl subtype with a higher affinity for glutamate, than that found with the homomeric receptors.

For *P. univalens* GLC-2/GLC-3, the glutamate concentration–response curve revealed an EC_{50} of 120.2 (109.2 – 132.3) µM ($n = 21$) whereas the EC_{50} for Pun-GLC-3 was 1482.2 (1275.6 – 1723.6) µM ($n = 11$) (Figure 5b). This 12-fold shift of EC_{50} values also confirmed that Pun-GLC-2/GLC-3 forms a novel subtype of heteromeric GluCl distinct from the Pun-GLC-3 channel.

In order to evaluate the involvement of GLC-2/GLC-3 as putative molecular targets for macrocyclic lactones, we focused our attention on ivermectin, moxidectin and eprinomectin representing the most commonly used anthelmintic macrocyclic lactones in equids and ruminants (i.e., ivermectin and moxidectin used for *Parascaris* sp. treatment; eprinomectin used for clade V parasites on lactating animals). Strikingly, whereas the Cel-GLC-2/GLC-3 receptor was activated by 1-µM ivermectin, moxidectin or eprinomectin, surprisingly, for *P. univalens*, none of the tested macrocyclic lactones induced a current (Figure 6). This last result was further confirmed using a wider

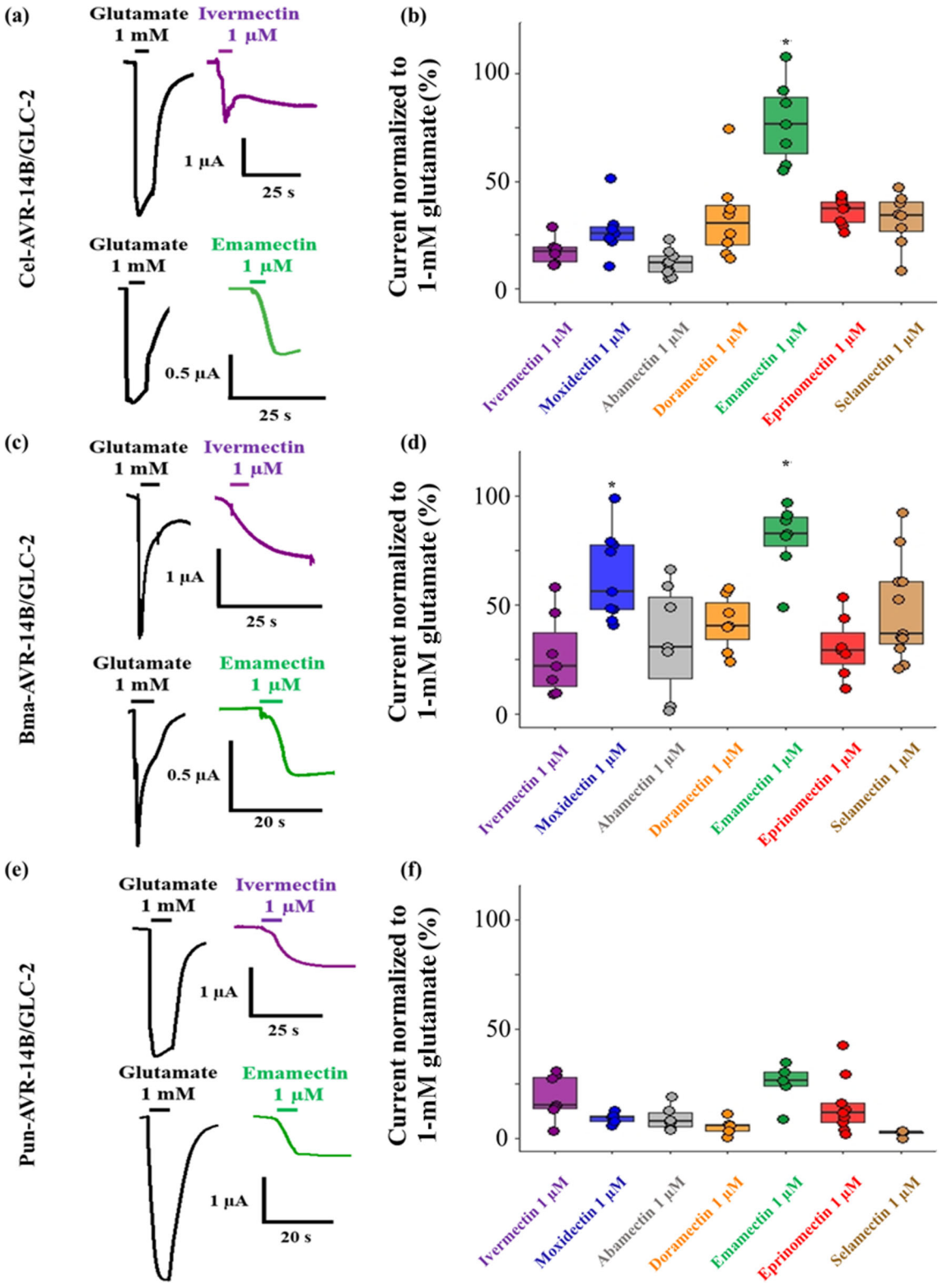

FIGURE 4 Effects of macrocyclic lactones on AVR-14B/GLC-2 receptors from *Caenorhabditis elegans*, *Brugia malayi* and *Parascaris univalens*. (a,c,e) Representative recording traces from a single oocyte injected with AVR-14B and GLC-2 of *C. elegans* (a), *B. malayi* (b) and *P. univalens* (c) induced by 1-µM ivermectin and 1-µM emamectin after a first application of 1-mM glutamate. Application times are indicated by the black bars. (b,d,f) Boxplots show the effects of the macrocyclic lactones (1 µM) after 5-s application on Cel-AVR-14B/GLC-2 (c), Bma-AVR-14B/GLC-2 (d) and Pun-AVR-14B/GLC-2 (e). All responses were normalized to the maximum responses obtained with glutamate at 1 mM. *$P < 0.05$, significantly different from effects of ivermectin

TABLE 1 Effect of 1-μM application of different macrocyclic lactones on *Caenorhabditis elegans*, *Brugia malayi* and *Parascaris univalens* AVR-14B/GLC-2 receptors

	IVM	MOX	ABA	DOR	EMA	EPR	SEL
C. elegans AVR-14B/GLC-2	17.6 ± 2.7 ($n = 6$)	27.3 ± 4.7 ($n = 7$)	11.9 ± 2.0 ($n = 9$)	33.4 ± 6.9 ($n = 8$)	77.7 ± 7.3 ($n = 7$)	35.9 ± 2.2 ($n = 8$)	32.0 ± 4.4 ($n = 8$)
B. malayi AVR-14B/GLC-2	27.0 ± 7.1 ($n = 7$)	63.1 ± 6.7 ($n = 9$)	34.1 ± 9.7 ($n = 7$)	41.8 ± 4.8 ($n = 7$)	80.5 ± 6.0 ($n = 7$)	30.8 ± 5.4 ($n = 7$)	47.9 ± 7.1 ($n = 11$)
P. univalens AVR-14B/GLC-2	19.0 ± 3.8 ($n = 7$)	9.3 ± 1.1 ($n = 5$)	9.4 ± 2.3 ($n = 6$)	5.4 ± 1.8 ($n = 5$)	24.9 ± 4.4 ($n = 5$)	15.1 ± 4.4 ($n = 9$)	2.5 ± 0.6 ($n = 5$)

Note: Values are means ± SEM, representing percentage of 1-mM glutamate-induced response.
Abbreviations: ABA, abamectin; DOR, doramectin; EMA, emamectin; EPR, eprinomectin; IVM, ivermectin; MOX, moxidectin; SEL, selamectin.

FIGURE 5 Glutamate concentration–response relationships for GLC-2/GLC-3 receptors from *Caenorhabditis elegans* and *Parascaris univalens*. (a,b) Glutamate concentration–response curves for *C. elegans* GLC-2 and the GLC-2/GLC-3 combination (a); *P. univalens* GLC-3 and the GLC-2/GLC-3 combination (b). Current amplitudes were normalized to the maximal effect obtained with glutamate. Solid line stands for the fitted log-logistic regression curve, and shaded area indicates 95% confidence interval. For both nematode species, the glutamate EC_{50} values were significantly different between the heteromeric and homomeric receptors

panel of macrocyclic lactones (Figure S5a). In order to investigate if the drug application time could potentially alter the effects of the macrocyclic lactone, 1-μM ivermectin was perfused for 90 s on Pun-GLC-2/GLC-3. Even with this long-lasting application, ivermectin remained poorly effective as an agonist with a median current amplitude corresponding to 0.37% ($n = 7$) of the maximum response obtained with glutamate (Figure S5b).

Because of this unexpected lack of activity as agonists, we hypothesized that the macrocyclic lactones could act both as antagonists or potentiators of the glutamate effect on Pun-GLC-2/GLC-3. In order to test this hypothesis, 100-μM glutamate (corresponding

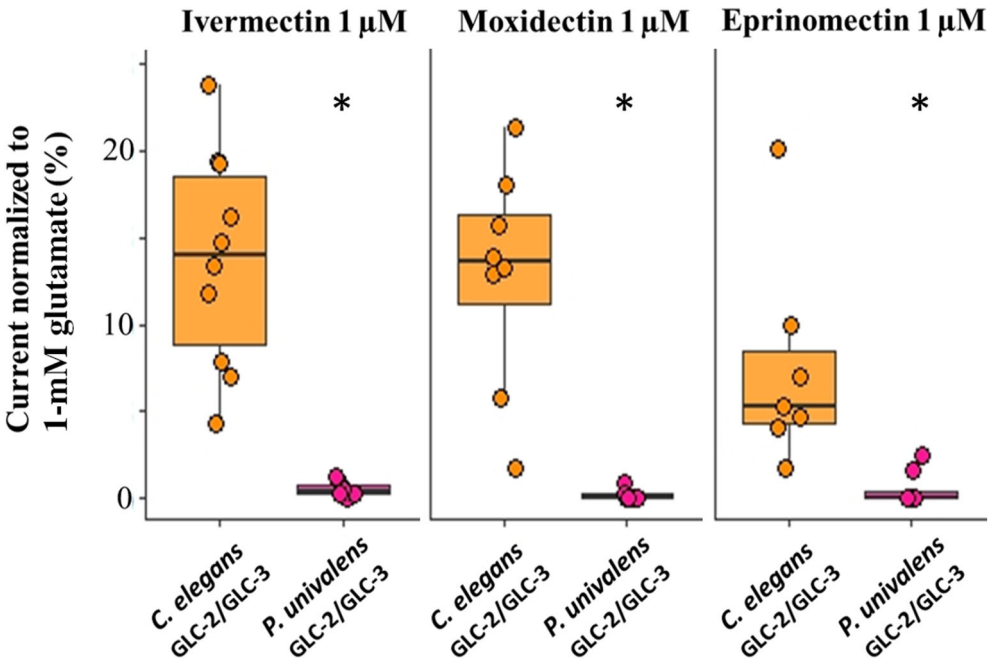

FIGURE 6 Effects of ivermectin, moxidectin and eprinomectin on GLC-2/GLC-3 receptors from *Caenorhabditis elegans* and *Parascaris univalens*. Boxplots depict 1-µM ivermectin, moxidectin or eprinomectin effects after 5-s application on GLC-2/GLC-3 from *C. elegans* and *P. univalens*. All currents were normalized to 1-mM glutamate-elicited currents. Ivermectin, moxidectin or eprinomectin applications induced higher currents in GLC-2/GLC-3 receptors from *C. elegans*. *$P < 0.05$, significantly different from *C. elegans*

approximately to the receptor glutamate EC_{50}) was applied before, during and after the addition of 1-µM ivermectin or moxidectin on the receptor (Figure 7a,b). Strikingly, both drugs potentiated the effects of glutamate on Pun-GLC-2/GLC-3. Median current amplitudes in response to 100-µM glutamate were increased by 50% ($n = 5$) and 75% ($n = 8$), when co-applied with ivermectin or moxidectin, respectively (Figure 7c,d). This effect was reversible for both ivermectin and moxidectin. Whereas it has been previously reported that concentrations of ivermectin that were too low to directly activate the channels would nonetheless potentiate the effects of glutamate (Cully et al., 1994), this is, to our knowledge, the first evidence of a nematode GluCl response potentiated by macrocyclic lactones at high concentrations, thus representing a novel receptor subtype with unique pharmacological properties.

4 | DISCUSSION

4.1 | Diversity of GluCls in distantly related nematodes

Among the six distinct genes encoding GluCl subunits in the free-living model nematode *C. elegans*, *avr-14*, *glc-2*, *glc-3* and *glc-4* are highly conserved in distantly related nematode species from different phylogenetic clades (Williamson et al., 2007). Here, we identified GluCls composed of the GLC-2, GLC-3 and AVR-14B subunits from *C. elegans*, *B. malayi* and *P. univalens*, two parasitic nematodes presenting a major impact for human and equine health, respectively. In *C. elegans*, we confirmed that homomeric receptors composed of AVR-14B or GLC-2 are responsive to glutamate in the µM range with elicited currents at the µA range, whereas, in contrast, the GLC-3 homomeric receptor only responds to mM glutamate application resulting in small currents at the nA range. Strikingly, for the latter, we showed that addition to GLC-2 led to the formation of a novel heteromeric GLC-2/GLC-3 receptor, responsive to more physiologically relevant glutamate concentrations. Even though it remains speculative to consider that such differences could reflect the existence of such a subunit combination in vivo, it clearly highlights the need to further investigate heteromeric GluCls in nematodes.

In clade V nematode species such as *H. contortus* (Atif et al., 2017, 2019) and *C. oncophora* (Njue et al., 2004), homomeric glutamate-sensitive channels made of AVR-14B or GLC-2 have also been described, suggesting that such recombinant homomeric GluCl channels could also be obtained from other parasitic nematode species. However, in the present study, we showed that none of the GluCl subunits from the parasites *B. malayi* or from *P. univalens* (i.e., AVR-14B, GLC-2, GLC-3 and GLC-4) gave rise to robust functional channels when expressed in the *Xenopus* oocytes (i.e., no glutamate elicited current, or small current at the nA range elicited by mM range glutamate). These results further supported the need to explore heteromeric GluCls in target parasitic species.

4.2 | The GLC-2 subunit is a key player for heteromeric GluCls

Previous studies reported that GLC-2 associates with GLC-1 or AVR-15 in *C. elegans* and with AVR-14B in *H. contortus* and *C. oncophora* (Atif et al., 2019; Cully et al., 1994; Njue et al., 2004; Vassilatis et al., 1997). In addition, the *C. elegans* AVR-14, GLC-2, GLC-3 and GLC-4 subunits have been shown to be expressed in pharyngeal neurons, suggesting potential interactions between these subunits in the worm (Cao et al., 2017; Hutter & Suh, 2016). It is noteworthy that the down-regulation of *glc-2* in *C. elegans* is embryonically lethal

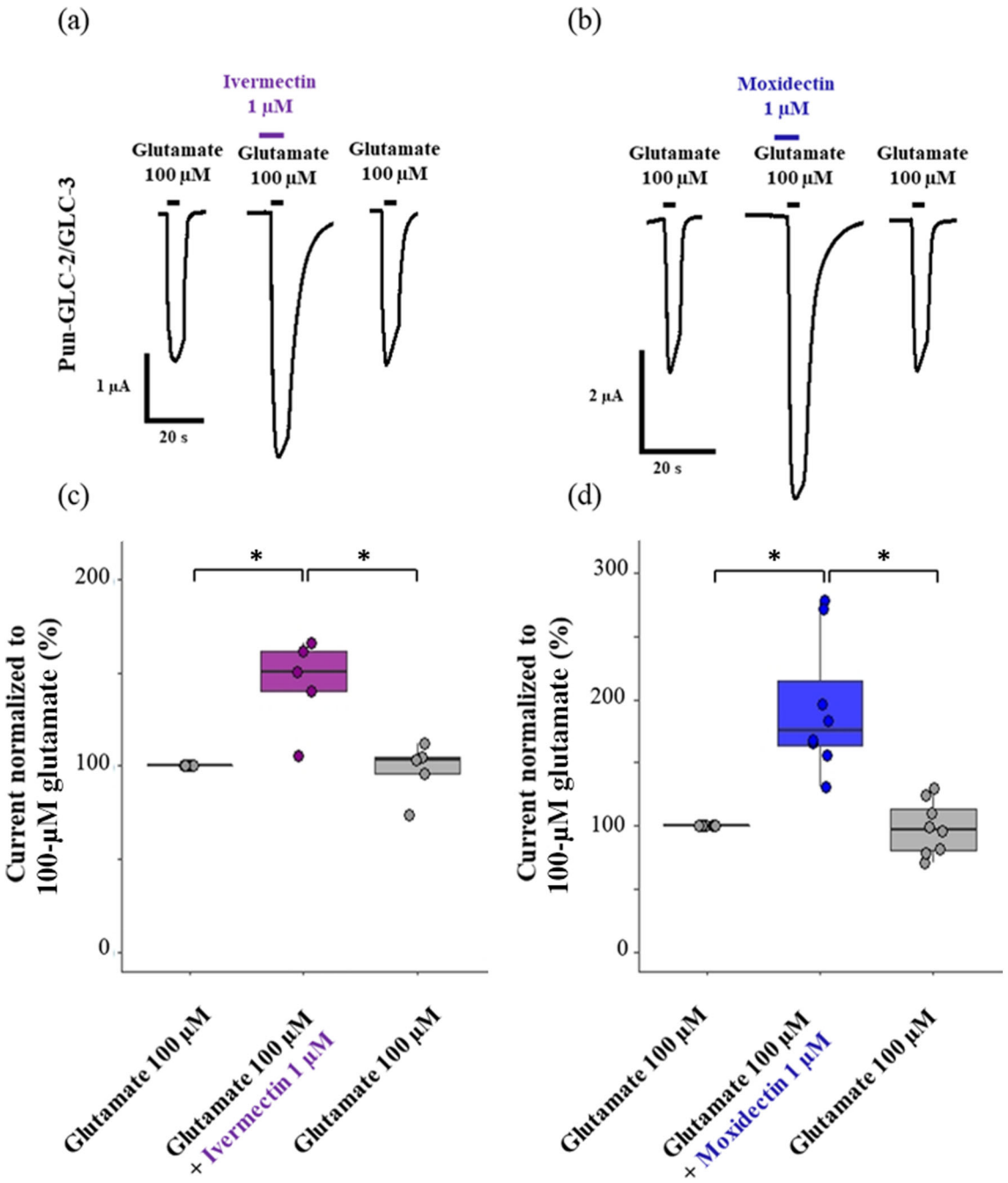

FIGURE 7 Modulation of glutamate effect by ivermectin and moxidectin on GLC-2/GLC-3 receptor from *Parascaris univalens*. (a,b) Representative current traces induced by glutamate 100 µM followed by a co-application of ivermectin 1 µM (a) or moxidectin 1 µM (b) with glutamate 100 µM and a final glutamate 100 µM application to monitor a potential reversible effect. Application times are indicated by the black bars. (c,d) Boxplots of summary data showing potentiating effect of ivermectin (c) and moxidectin (d) on Pun-GLC-2/GLC-3 normalized and compared with the response to 100-µM glutamate. Note that the effects of the macrocyclic lactones were reversible on washout. *$P < 0.05$, significantly different as indicated

(Sonnichsen et al., 2005) and that the *avr-14*, *avr-15*, *glc-1* triple mutant displays only subtle behavioural changes and is resistant to 4 µg·ml^{-1} ivermectin (Dent et al., 2000). Interestingly, the *avr-14*, *avr-15*, *glc-1*, *glc-3* quadruple mutant strain is also viable, fertile with very subtle phenotype but is able to survive up to 50 µg·ml^{-1} ivermectin exposure (Wever et al., 2015). Taken together, these data clearly support a major role for the GLC-2 subunit in *C. elegans* but also highlight GLC-3 as an important contributor to ivermectin susceptibility.

For *C. elegans*, *B. malayi* and *P. univalens*, the combination of AVR-14B/GLC-2 led to the robust expression of glutamate-sensitive receptors. The drastic reduction of the glutamate EC_{50} of AVR-14B/GLC-2 in comparison with their respective homomeric receptors strongly

support the association of the two distinct subunits into functional heteromeric receptors. Subsequently, we describe for the first time that GLC-2 and GLC-3 can associate to form a novel glutamate-sensitive channel subtype in *C. elegans* and *P. univalens*, but surprisingly not in *B. malayi*. Although the Bma-GLC-2 and Bma-GLC-3 subunits were shown to be functional with Bma-AVR-14B and Pun-GLC-2, respectively, they did not give rise to a heteromeric GluCl. Therefore, we can only speculate that additional subunits combining to GLC-3 alone or GLC-2/GLC-3 of *B. malayi* are required to form functional receptors. In addition, we cannot exclude that ancillary proteins might be required for the functional expression of GluCl receptor in *Xenopus* oocytes as reported for some ACh-receptor subtypes (Boulin et al., 2008, 2011; Courtot et al., 2015). Interestingly, as in *C. elegans*, the *glc-3* gene is present in *H. contortus* and *C. oncophora*, but the heteromeric combination with GLC-2 has never been tried so far. Therefore, the present study opens the way for the characterization of the new GLC-2/GLC-3 receptor subtype in other nematode species. In summary, our results highlight that subunit combination is critical for clade III parasites to form functional GluCls system but also contribute to the diversity of GluCl subtypes in clade V nematodes, including the model species *C. elegans*.

4.3 | New insights into the mode of action of macrocyclic lactones in *C. elegans* and parasitic nematodes

In accordance with previous studies performed on AVR-14B/GLC-2 of *H. contortus* (Atif et al., 2019) and *C. oncophora* (Njue et al., 2004), we showed that AVR-14B/GLC-2 from *C. elegans*, *B. malayi* and *P. univalens* were sensitive to ivermectin and moxidectin, corresponding to the two macrocyclic lactones with marketing authorization in human health (de Moraes & Geary, 2020) and the most widely used in equine health with abamectin and doramectin (Gokbulut & McKellar, 2018).

In addition, we showed that this GluCl subtype is also sensitive to a wide range of macrocyclic lactones including abamectin, doramectin, emamectin, eprinomectin and selamectin. Presently, only ivermectin has marketing authorization for a wide variety of hosts and parasites. Other macrocyclic lactones have more specific authorization, such as emamectin, which is mostly used as an insecticide in veterinarian aquaculture as well as in terrestrial agriculture (Lees et al., 2008). Interestingly, the present work highlights emamectin as a more potent agonist than ivermectin on the AVR-14B/GLC-2 receptors from *C. elegans* and *B. malayi*. However, whether the high potency of emamectin on AVR-14B/GLC-2 could be correlated or not with an efficacy of this drug on the worms remains to be established. Interestingly, this also raises the question of the relative contribution of the different nematode GluCl subtypes in the sensitivity to macrocyclic lactones. Here, we report a new subtype of functional GluCls made of GLC-2/GLC-3 in *C. elegans* and *P. univalens*. However, depending on the nematode species, they presented very contrasting pharmacological properties. For *C. elegans*, ivermectin, moxidectin and eprinomectin acted as agonists on GLC-2/GLC-3, thus underpinning a potential role for this heteromeric channel in its sensitivity to MLs. In that respect, our results provide an explanation for the drastic increase of ivermectin resistance in the *avr-14*, *avr-15*, *glc-1*, *glc-3* quadruple mutant in comparison with the *avr-14*, *avr-15*, *glc-1* triple mutant (Dent et al., 2000; Wever et al., 2015). In sharp contrast, for *P. univalens*, ivermectin, moxidectin and eprinomectin potentiated glutamate effect on its GLC-2/GLC-3 receptor. Such differences in pharmacological properties between nematode species highlight the need for future investigations of GLC-2/GLC-3 in other parasitic species as it could provide important information about amino acids involved in the receptor binding sites.

Interestingly, in some case of ivermectin resistance, moxidectin remains effective to treat lambs infected with *H. contortus* (Williamson et al., 2011), suggesting that each molecule could preferentially activate distinct pharmacological targets in the worms. Because stable transformation remains an elusive goal for numerous parasitic nematode species (Boyle & Yoshino, 2003; Selkirk et al., 2012), RNAi experiments could represent an attractive alternative to investigate the respective role of the distinct GluCls subtype in determining the susceptibility to macrocyclic lactones (Blanchard et al., 2018). RNAi has been successfully developed in *B. malayi* (Song et al., 2010) and in the pig nematode parasite *Ascaris suum* that is closely related to *P. univalens* (McCoy et al., 2015). Undoubtedly, such an approach combined with phenotypic assays (Storey et al., 2014) or the recently developed in vivo imaging system (IVIS) optimized to study *B. malayi* on jird (Liu et al., 2020) would represent a major opportunity to investigate in more detail the putative contribution of AVR-14B/GLC-2 and GLC-2/GLC-3 GluCl subtypes in the sensitivity to macrocyclic lactones.

In conclusion, our study provides new insight about the GluCl diversity and highlights the importance of GLC-2 as a core subunit in heteromeric GluCls from *C. elegans* and the clade III nematodes *B. malayi* and *P. univalens*. This work opens the way for the systematic investigation of heteromeric GluCl subtypes in target parasitic species in order to lay a strong basis for the rational use of macrocyclic lactones and the discovery of novel drug targets for the development of next generation anthelmintics.

ACKNOWLEDGEMENTS

We thank Prof. Adrian Wolstenholme from the Department of Infectious Diseases, College of Veterinary Medicine, University of Georgia, Athens, GA 30602, USA, for providing the *Brugia malayi* worms and the careful and critical reading of the manuscript. We thank the group of UEPAO (Experimental Unit of Orfrasière Animal Physiology, INRAE Centre Val de Loire, Nouzilly 37380, France) for providing *Parascaris univalens* eggs and adults. N.L. is the grateful recipient of a PhD grant from the Animal Health Division of INRAE and from the Region Centre-Val de Loire, France. N.L. was supported by a grant from the RTR Fédération de Recherche en Infectiologie (https://www.infectiologie-regioncentre.fr/) of the Région Centre-Val de Loire. The funders had no role in study design, data collection and analysis, decision to publish or preparation of the manuscript.

AUTHOR CONTRIBUTIONS

N.L., E.C. and C.L.C. performed the experiments and analysed the two-electrode voltage-clamp data; N.L. and A.C. performed molecular biology; N.L., C.L.C. and C.N. designed the study; and N.L., E.C., C.L.C. and C.N. interpreted data and drafted the manuscript.

DECLARATION OF TRANSPARENCY AND SCIENTIFIC RIGOUR

This Declaration acknowledges that this paper adheres to the principles for transparent reporting and scientific rigour of preclinical research as stated in the *BJP* guidelines for Design & Analysis, and as recommended by funding agencies, publishers and other organizations engaged with supporting research.

DATA AVAILABILITY STATEMENT

The data that support the findings of this study are available from the corresponding author upon reasonable request. Some data may not be made available because of privacy or ethical restrictions.

ORCID

Nicolas Lamassiaude https://orcid.org/0000-0002-2470-9490
Elise Courtot https://orcid.org/0000-0003-0937-6218
Angélique Corset https://orcid.org/0000-0003-2140-4656
Claude L. Charvet https://orcid.org/0000-0002-0596-6598
Cédric Neveu https://orcid.org/0000-0003-4314-1850

REFERENCES

Alexander, S. P., Mathie, A., Peters, J. A., Veale, E. L., Striessnig, J., Kelly, E., Armstrong, J. F., Faccenda, E., Harding, S. D., Pawson, A. J., Southan, C., Davies, J. A., Aldrich, R. W., Attali, B., Baggetta, A. M., Becirovic, E., Biel, M., Bill, R. M., Catterall, W. A., … Zhu, M. (2021). THE CONCISE GUIDE TO PHARMACOLOGY 2021/22: Ion channels. *British Journal of Pharmacology*, *178*(S1), S157–S245. https://doi.org/10.1111/bph.15539

Atif, M., Estrada-Mondragon, A., Nguyen, B., Lynch, J. W., & Keramidas, A. (2017). Effects of glutamate and ivermectin on single glutamate-gated chloride channels of the parasitic nematode *H. contortus*. *PLoS Pathogens*, *13*, e1006663. https://doi.org/10.1371/journal.ppat.1006663

Atif, M., Smith, J. J., Estrada-Mondragon, A., Xiao, X., Salim, A. A., Capon, R. J., Lynch, J. W., & Keramidas, A. (2019). GluClR-mediated inhibitory postsynaptic currents reveal targets for ivermectin and potential mechanisms of ivermectin resistance. *PLoS Pathogens*, *15*(1), e1007570. https://doi.org/10.1371/journal.ppat.1007570

Beech, R. N., Wolstenholme, A. J., Neveu, C., & Dent, J. A. (2010). Nematode parasite genes: What's in a name? *Trends in Parasitology*, *26*(7), 334–340. https://doi.org/10.1016/j.pt.2010.04.003

Bendtsen, J. D., Nielsen, H., von Heijne, G., & Brunak, S. (2004). Improved prediction of signal peptides: SignalP 3.0. *Journal of Molecular Biology*, *340*(4), 783–795. pmid:15223320. https://doi.org/10.1016/j.jmb.2004.05.028

Bianchi, L., & Driscoll, M. (2006). Heterologous expression of *C. elegans* ion channels in Xenopus oocytes. *WormBook*, 1–16. https://doi.org/10.1895/wormbook.1.117.1

Blanchard, A., Guegnard, F., Charvet, C. L., Crisford, A., Courtot, E., Sauve, C., Harmache, A., Duguet, T., O'Connor, V., Castagnone-Sereno, P., Reaves, B., Wolstenholme, A. J., Beech, R. N., Holden-Dye, L., & Neveu, C. (2018). Deciphering the molecular determinants of cholinergic anthelmintic sensitivity in nematodes: When novel functional validation approaches highlight major differences between the model *Caenorhabditis elegans* and parasitic species. *PLoS Pathogens*, *14*(5), e1006996. https://doi.org/10.1371/journal.ppat.1006996

Blaxter, M., & Koutsovoulos, G. (2015). The evolution of parasitism in Nematoda. *Parasitology*, *142*(Suppl 1), S26–S39. https://doi.org/10.1017/S0031182014000791

Blaxter, M. L., De Ley, P., Garey, J. R., Liu, L. X., Scheldeman, P., Vierstraete, A., Vanfleteren, J. R., Mackey, L. Y., Dorris, M., Frisse, L. M., Vida, J. T., & Thomas, W. K. (1998). A molecular evolutionary framework for the phylum Nematoda. *Nature*, *392*(6671), 71–75. https://doi.org/10.1038/32160

Boulin, T., Fauvin, A., Charvet, C. L., Cortet, J., Cabaret, J., Bessereau, J. L., & Neveu, C. (2011). Functional reconstitution of *Haemonchus contortus* acetylcholine receptors in *Xenopus* oocytes provides mechanistic insights into levamisole resistance. *British Journal of Pharmacology*, *164*(5), 1421–1432. https://doi.org/10.1111/j.1476-5381.2011.01420.x

Boulin, T., Gielen, M., Richmond, J. E., Williams, D. C., Paoletti, P., & Bessereau, J. L. (2008). Eight genes are required for functional reconstitution of the *Caenorhabditis elegans* levamisole-sensitive acetylcholine receptor. *Proceedings of the National Academy of Sciences of the United States of America*, *105*(47), 18590–18595. https://doi.org/10.1073/pnas.0806933105

Boyle, J. P., & Yoshino, T. P. (2003). Gene manipulation in parasitic helminths. *International Journal for Parasitology*, *33*(11), 1259–1268. https://doi.org/10.1016/s0020-7519(03)00159-0

Campbell, W. C. (2012). History of avermectin and ivermectin, with notes on the history of other macrocyclic lactone antiparasitic agents. *Current Pharmaceutical Biotechnology*, *13*(6), 853–865. https://doi.org/10.2174/138920112800399095

Cao, J., Packer, J. S., Ramani, V., Cusanovich, D. A., Huynh, C., Daza, R., Qiu, X., Lee, C., Furlan, S. N., Steemers, F. J., Adey, A., Waterston, R. H., Trapnell, C., & Shendure, J. (2017). Comprehensive single-cell transcriptional profiling of a multicellular organism. *Science*, *357*(6352), 661–667. https://doi.org/10.1126/science.aam8940

Charvet, C. L., Guegnard, F., Courtot, E., Cortet, J., & Neveu, C. (2018). Nicotine-sensitive acetylcholine receptors are relevant pharmacological targets for the control of multidrug resistant parasitic nematodes. *International Journal for Parasitology: Drugs and Drug Resistance*, *8*(3), 540–549. https://doi.org/10.1016/j.ijpddr.2018.11.003

Cheeseman, C. L., Delany, N. S., Woods, D. J., & Wolstenholme, A. J. (2001). High-affinity ivermectin binding to recombinant subunits of the *Haemonchus contortus* glutamate-gated chloride channel. *Molecular and Biochemical Parasitology*, *114*(2), 161–168. https://doi.org/10.1016/s0166-6851(01)00258-4

Cook, A., Aptel, N., Portillo, V., Siney, E., Sihota, R., Holden-Dye, L., & Wolstenholme, A. (2006). *Caenorhabditis elegans* ivermectin receptors regulate locomotor behaviour and are functional orthologues of *Haemonchus contortus* receptors. *Molecular and Biochemical Parasitology*, *147*(1), 118–125. https://doi.org/10.1016/j.molbiopara.2006.02.003

Courtot, E., Charvet, C. L., Beech, R. N., Harmache, A., Wolstenholme, A. J., Holden-Dye, L., O'Connor, V., Peineau, N., Woods, D. J., & Neveu, C. (2015). Functional characterization of a novel class of morantel-sensitive acetylcholine receptors in nematodes. *PLoS Pathogens*, *11*(12), e1005267. https://doi.org/10.1371/journal.ppat.1005267

Cully, D. F., Vassilatis, D. K., Liu, K. K., Paress, P. S., Van der Ploeg, L. H., Schaeffer, J. M., & Arena, J. P. (1994). Cloning of an avermectin-sensitive glutamate-gated chloride channel from *Caenorhabditis elegans*. *Nature*, *371*(6499), 707–711. https://doi.org/10.1038/371707a0

Cully, D. F., Wilkinson, H., & Vassilatis, D. K. (1996). Molecular biology and electrophysiology of glutamate-gated chloride channels of invertebrates. *Parasitology*, *113*, S191–S200. https://doi.org/10.1017/S0031182000077970

Curtis, M. J., Alexander, S. P. H., Cirino, G., Docherty, J. R., George, C. H., Giembycz, M. A., Hoyer, D., Insel, P. A., Izzo, A. A., Ji, Y., MacEwan, D. J., Sobey, C. G., Stanford, S. C., Teixeira, M. M., Wonnacott, S., & Ahluwalia, A. (2018). Experimental design and analysis and their reporting II: updated and simplified guidance for authors and peer reviewers. *British Journal of Pharmacology*, *175*, 987–993. https://doi.org/10.1111/bph.14153

de Moraes, J., & Geary, T. G. (2020). FDA-approved antiparasitic drugs in the 21st century: A success for helminthiasis? *Trends in Parasitology*, *36*(7), 573–575. https://doi.org/10.1016/j.pt.2020.04.005

Degani-Katzav, N., Gortler, R., Gorodetzki, L., & Paas, Y. (2016). Subunit stoichiometry and arrangement in a heteromeric glutamate-gated chloride channel. *Proceedings of the National Academy of Sciences of the United States of America*, *113*(5), E644–E653. https://doi.org/10.1073/pnas.1423753113

Dent, J. A., Davis, M. W., & Avery, L. (1997). avr-15 encodes a chloride channel subunit that mediates inhibitory glutamatergic neurotransmission and ivermectin sensitivity in *Caenorhabditis elegans*. *The EMBO Journal*, *16*(19), 5867–5879. https://doi.org/10.1093/emboj/16.19.5867

Dent, J. A., Smith, M. M., Vassilatis, D. K., & Avery, L. (2000). The genetics of ivermectin resistance in *Caenorhabditis elegans*. *Proceedings of the National Academy of Sciences of the United States of America*, *97*(6), 2674–2679. https://doi.org/10.1073/pnas.97.6.2674

Global programme to eliminate lymphatic filariasis: progress report, 2016. (2017). *Weekly Epidemiological Record*, *92*(40), 594–607.

Gokbulut, C., & McKellar, Q. A. (2018). Anthelmintic drugs used in equine species. *Veterinary Parasitology*, *261*, 27–52. https://doi.org/10.1016/j.vetpar.2018.08.002

Gouy, M., Guindon, S., & Gascuel, O. (2010). SeaView version 4: A multiplatform graphical user Interface for sequence alignment and phylogenetic tree building. *Molecular Biology and Evolution*, *27*(2), 221–224. https://doi.org/10.1093/molbev/msp259

Hernando, G., & Bouzat, C. (2014). *Caenorhabditis elegans* neuromuscular junction: GABA receptors and ivermectin action. *PLoS ONE*, *9*(4), e95072. https://doi.org/10.1371/journal.pone.0095072

Hibbs, R. E., & Gouaux, E. (2011). Principles of activation and permeation in an anion-selective Cys-loop receptor. *Nature*, *474*(7349), 54–60. https://doi.org/10.1038/nature10139

Holden-Dye, L., & Walker, R. J. (2006). Actions of glutamate and ivermectin on the pharyngeal muscle of *Ascaridia galli*: A comparative study with *Caenorhabditis elegans*. *International Journal for Parasitology*, *36*(4), 395–402. https://doi.org/10.1016/j.ijpara.2005.11.006

Horoszok, L., Raymond, V., Sattelle, D. B., & Wolstenholme, A. J. (2001). GLC-3: A novel fipronil and BIDN-sensitive, but picrotoxinin-insensitive, L-glutamate-gated chloride channel subunit from *Caenorhabditis elegans*. *British Journal of Pharmacology*, *132*(6), 1247–1254. https://doi.org/10.1038/sj.bjp.0703937

Hutter, H., & Suh, J. (2016). GExplore 1.4: An expanded web interface for queries on *Caenorhabditis elegans* protein and gene function. *Worm*, *5*, e1234659. https://doi.org/10.1080/21624054.2016.1234659

Kaplan, R. M., & Vidyashankar, A. N. (2012). An inconvenient truth: Global worming and anthelmintic resistance. *Veterinary Parasitology*, *186*(1–2), 70–78. https://doi.org/10.1016/j.vetpar.2011.11.048

Laing, R., Gillan, V., & Devaney, E. (2017). Ivermectin—Old drug, new tricks? *Trends in Parasitology*, *33*(6), 463–472. https://doi.org/10.1016/j.pt.2017.02.004

Lamassiaude, N., Toubate, B., Neveu, C., Charnet, P., Neveu, C., Dupuy, C., Debierre-Grockiego, F., Dimier-Poisson, I., & Charvet, C. L. (2021). The molecular targets of ivermectin and lotilaner in the human louse *Pediculus humanus humanus*: New prospects for the treatment of pediculosis. *PLoS Pathogens*, *17*(2), e1008863. https://doi.org/10.1371/journal.ppat.1008863

Lees, F., Baillie, M., Gettinby, G., & Revie, C. W. (2008). The efficacy of emamectin benzoate against infestations of *Lepeophtheirus salmonis* on farmed Atlantic salmon (*Salmo salar* L) in Scotland, 2002–2006. *PLoS ONE*, *3*(2), e1549. https://doi.org/10.1371/journal.pone.0001549

Liu, C., De, S. L., Miley, K., & Unnasch, T. R. (2020). In vivo imaging of transgenic *Brugia malayi*. *PLoS Neglected Tropical Diseases*, *14*(4), e0008182. https://doi.org/10.1371/journal.pntd.0008182

Madeira, F., Park, Y. M., Lee, J., Buso, N., Gur, T., Madhusoodanan, N., Basutkar, P., Tivey, A. R., Potter, S. C., Finn, R. D., & Lopez, R. (2019). The EMBL-EBI search and sequence analysis tools APIs in 2019. *Nucleic Acids Research*, *47*, 636–641. https://doi.org/10.1093/nar/gkz268

Martin, F., Hoglund, J., Bergstrom, T. F., Karlsson Lindsjo, O., & Tyden, E. (2018). Resistance to pyrantel embonate and efficacy of fenbendazole in *Parascaris univalens* on Swedish stud farms. *Veterinary Parasitology*, *264*, 69–73. https://doi.org/10.1016/j.vetpar.2018.11.003

Matthews, J. B., Geldhof, P., Tzelos, T., & Claerebout, E. (2016). Progress in the development of subunit vaccines for gastrointestinal nematodes of ruminants. *Parasite Immunology*, *38*(12), 744–753. https://doi.org/10.1111/pim.12391

McCavera, S., Rogers, A. T., Yates, D. M., Woods, D. J., & Wolstenholme, A. J. (2009). An ivermectin-sensitive glutamate-gated chloride channel from the parasitic nematode *Haemonchus contortus*. *Molecular Pharmacology*, *75*(6), 1347–1355. https://doi.org/10.1124/mol.108.053363

McCoy, C. J., Warnock, N. D., Atkinson, L. E., Atcheson, E., Martin, R. J., Robertson, A. P., Maule, A. G., Marks, N. J., & Mousley, A. (2015). RNA interference in adult *Ascaris suum*—An opportunity for the development of a functional genomics platform that supports organism-, tissue- and cell-based biology in a nematode parasite. *International Journal for Parasitology*, *45*(11), 673–678. https://doi.org/10.1016/j.ijpara.2015.05.003

Nielsen, M. K., Wang, J., Davis, R., Bellaw, J. L., Lyons, E. T., Lear, T. L., & Goday, C. (2014). *Parascaris univalens*—A victim of large-scale misidentification? *Parasitology Research*, *113*(12), 4485–4490. https://doi.org/10.1007/s00436-014-4135-y

Njue, A. I., Hayashi, J., Kinne, L., Feng, X. P., & Prichard, R. K. (2004). Mutations in the extracellular domains of glutamate-gated chloride channel α3 and β subunits from ivermectin-resistant *Cooperia oncophora* affect agonist sensitivity. *Journal of Neurochemistry*, *89*(5), 1137–1147. https://doi.org/10.1111/j.1471-4159.2004.02379.x

Peregrine, A. S., Molento, M. B., Kaplan, R. M., & Nielsen, M. K. (2014). Anthelmintic resistance in important parasites of horses: Does it really matter? *Veterinary Parasitology*, *201*(1–2), 1–8. https://doi.org/10.1016/j.vetpar.2014.01.004

Pullan, R. L., Smith, J. L., Jasrasaria, R., & Brooker, S. J. (2014). Global numbers of infection and disease burden of soil transmitted helminth infections in 2010. *Parasites & Vectors*, *7*, 37. https://doi.org/10.1186/1756-3305-7-37

Ramaiah, K. D., & Ottesen, E. A. (2014). Progress and impact of 13 years of the global programme to eliminate lymphatic filariasis on reducing the burden of filarial disease. *PLoS Neglected Tropical Diseases*, *8*(11), e3319. https://doi.org/10.1371/journal.pntd.0003319

Reinemeyer, C. R., & Nielsen, M. K. (2009). Parasitism and colic. *The Veterinary Clinics of North America. Equine Practice*, *25*(2), 233–245. https://doi.org/10.1016/j.cveq.2009.04.003

Salle, G., Guillot, J., Tapprest, J., Foucher, N., Sevin, C., & Laugier, C. (2020). Compilation of 29 years of postmortem examinations identifies major shifts in equine parasite prevalence from 2000 onwards. *International Journal for Parasitology*, *50*(2), 125–132. https://doi.org/10.1016/j.ijpara.2019.11.004

Schultz, J., Milpetz, F., Bork, P., & Ponting, C. P. (1998). SMART, a simple modular architecture research tool: Identification of signaling domains. *Proceedings of the National Academy of Sciences of the United States of America*, *95*(11), 5857–5864. pmid:9600884. https://doi.org/10.1073/pnas.95.11.5857

Selkirk, M. E., Huang, S. C., Knox, D. P., & Britton, C. (2012). The development of RNA interference (RNAi) in gastrointestinal nematodes. *Parasitology*, *139*(5), 605–612. https://doi.org/10.1017/S0031182011002332

Song, C., Gallup, J. M., Day, T. A., Bartholomay, L. C., & Kimber, M. J. (2010). Development of an in vivo RNAi protocol to investigate gene function in the filarial nematode, *Brugia malayi*. *PLoS Pathogens*, *6*(12), e1001239. https://doi.org/10.1371/journal.ppat.1001239

Sonnichsen, B., Koski, L. B., Walsh, A., Marschall, P., Neumann, B., Brehm, M., Alleaume, A.-M., Artelt, J., Bettencourt, P., Cassin, E., Hewitson, M., Holz, C., Khan, M., Lazik, S., Martin, C., Nitzsche, B., Ruer, M., Stamford, J., Winzi, M., … Echeverri, C. J. (2005). Full-genome RNAi profiling of early embryogenesis in *Caenorhabditis elegans*. *Nature*, *434*(7032), 462–469. https://doi.org/10.1038/nature03353

Storey, B., Marcellino, C., Miller, M., Maclean, M., Mostafa, E., Howell, S., Sakanari, J., Wolstenholme, A., & Kaplan, R. (2014). Utilization of computer processed high definition video imaging for measuring motility of microscopic nematode stages on a quantitative scale: "The Worminator". *International Journal for Parasitology: Drugs and Drug Resistance*, *4*(3), 233–243. https://doi.org/10.1016/j.ijpddr.2014.08.003

Vassilatis, D. K., Arena, J. P., Plasterk, R. H., Wilkinson, H. A., Schaeffer, J. M., Cully, D. F., & Van der Ploeg, L. H. (1997). Genetic and biochemical evidence for a novel avermectin-sensitive chloride channel in *Caenorhabditis elegans*. Isolation and characterization. *The Journal of Biological Chemistry*, *272*(52), 33167–33174. https://doi.org/10.1074/jbc.272.52.33167

Wever, C. M., Farrington, D., & Dent, J. A. (2015). The validation of nematode-specific acetylcholine-gated chloride channels as potential anthelmintic drug targets. *PLoS ONE*, *10*(9), e0138804. https://doi.org/10.1371/journal.pone.0138804

Williamson, S. M., Storey, B., Howell, S., Harper, K. M., Kaplan, R. M., & Wolstenholme, A. J. (2011). Candidate anthelmintic resistance-associated gene expression and sequence polymorphisms in a triple-resistant field isolate of *Haemonchus contortus*. *Molecular and Biochemical Parasitology*, *180*(2), 99–105. https://doi.org/10.1016/j.molbiopara.2011.09.003

Williamson, S. M., Walsh, T. K., & Wolstenholme, A. J. (2007). The cys-loop ligand-gated ion channel gene family of *Brugia malayi* and *Trichinella spiralis*: A comparison with *Caenorhabditis elegans*. *Invertebrate Neuroscience*, *7*(4), 219–226. https://doi.org/10.1007/s10158-007-0056-0

Yates, D. M., & Wolstenholme, A. J. (2004). An ivermectin-sensitive glutamate-gated chloride channel subunit from *Dirofilaria immitis*. *International Journal for Parasitology*, *34*(9), 1075–1081. https://doi.org/10.1016/j.ijpara.2004.04.010

SUPPORTING INFORMATION

Additional supporting information may be found in the online version of the article at the publisher's website.

How to cite this article: Lamassiaude, N., Courtot, E., Corset, A., Charvet, C. L., & Neveu, C. (2022). Pharmacological characterization of novel heteromeric GluCl subtypes from *Caenorhabditis elegans* and parasitic nematodes. *British Journal of Pharmacology*, *179*(6), 1264–1279. https://doi.org/10.1111/bph.15703